Temporal Seismic Velocity Variations: Recovery Following from the 2019 Mw 7.1 Ridgecrest Earthquake

Joshua Boschelli[1,2]; Morgan P. Moschetti[1]; Christoph Sens-Schonfelder[3]

[1]Geologic Hazards Science Center, U.S. Geological Survey, Golden, CO, USA, [2]Department of Earth and Atmospheric Sciences, Saint Louis University, St. Louis, MO, USA, [3]Helmholtz Centre Potsdam—GFZ German Research Centre for Geosciences, Potsdam, Germany

SCEC AN NSF+USGS CENTER

Abstract

We investigated seismic velocity changes (*dv/v*) associated with the 2019 Ridgecrest earthquake sequence from high-frequency autocorrelations of ambient seismic noise data. Daily autocorrelation functions were computed for the entirety of 2019 and early 2020 for the permanent broadband stations within the region that experienced strong ground shaking, defined by peak ground accelerations of greater than 10 percent of *g* during the M_w 7.1 earthquake, and for the temporary broadband stations installed during the aftershock deployment. Travel time shifts in the daily autocorrelation functions, relative to the mean autocorrelation waveform, were computed to produce *dv/v* time series, which are sensitive to the evolving material properties of the shallow crust surrounding the Ridgecrest fault zone (RFZ). A short-term velocity drop follows the M_w 7.1 earthquake at stations in the vicinity of the M_w 7.1 earthquake, while those greater than 50 km away showed no such drop despite recording peak ground accelerations of up to more than 22 percent of *g*. Additionally, the maximum, absolute seismic velocity changes are proportional to the logarithm of distance from the fault rupture. Seismic velocity changes exhibit a weak correlation with peak horizontal ground accelerations, and better correlations exists between the seismic velocity, two distinctive temporal behaviors emerged. Near the RFZ fault surface, seismic velocities recovered over 7 months and may continue to do so. However, in the vicinity of the nearby Garlock fault, where triggered slip manifested, and north of the RFZ, seismic velocities recovered over a much shorter time period (about 1 month). We interpret the seismic velocity changes and their recovery to be largely due to changes in the physical properties of the shallow crust, such as fault zone damage recovery caused by the earthquake rupture process, and perhaps in response to the large dynamic stresses of passing seismic waves.

Data and Methodology

We collected continuous data from 16 broadband seismographs from the Southern California Seismic Networks, including the permanent (CI) network and temporary, portable network (ZY) deployed immediately after the M_w 7.1 earthquake (Figure 1). Fifteen months of continuous seismic data, spanning all of 2019 and the first quarter of 2020, provides a useful set of measurements for the region. Since the ZY stations were deployed in response to the M_w 7.1 Ridgecrest event, their coverage begins after the mainshock; however, measurements from the temporary deployment provide useful constraints on the evolution of seismic velocities in the months following their installation, particularly at sites near the rupture (Cochran et al., 2020).

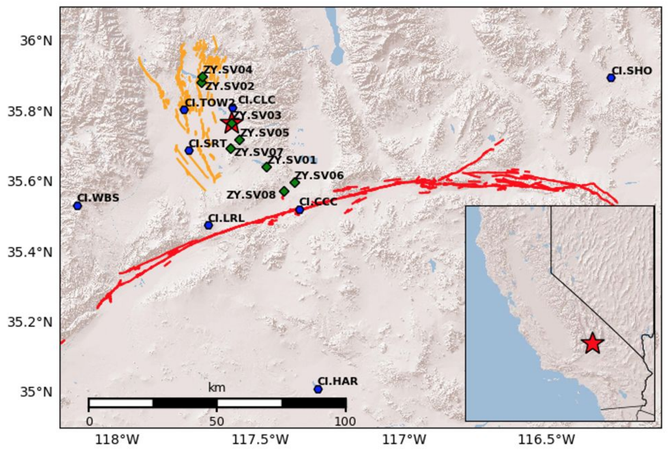

Figure 1: Locations of the permanent and temporary seismic stations relative to the M_w 7.1 Ridgecrest earthquake with the local fault networks shown, the Ridgecrest fault zone (orange) and the Garlock fault (red). Permanent stations of the CI network (blue hexagon), Temporary seismic stations of the ZY network (green diamond), and the epicenter of the Ridgecrest earthquake (red star).

To quantify the temporal variation of the seismic velocity, we adopted the techniques of Passive Image Interferometry as pioneered by Sens-Schönfelder and Wegler (2006) and applied them to autocorrelations across the six different combinations of the instruments components. The relative travel time variations are calculated by computing a reference autocorrelation Φ_{ref} for each station and then comparing the stretched and compressed daily autocorrelations that maximizes their correlation coefficient. This stretching factors, ε , relates to the temporal velocity variations by:

$$coef(\mathcal{E},t) = \frac{\int_{t_1}^{t_2} \Phi_d\big(t(1+\mathcal{E})\big)\Phi_{ref}(t)dt}{\left(\int_{t_1}^{t_2} \Phi_d^2\big(t(1+\mathcal{E})\big)dt \int_{t_1}^{t_2} \Phi_{ref}^2(t)dt\right)^{\frac{1}{2}}} \qquad \varepsilon(t) = \frac{\Delta t}{t} = \frac{-dv}{v}$$

Temporal Evolution of the Autocorrelation Waveforms

Matrices of the daily autocorrelations can provide initial information on the effect of the M_w 7.1 Ridgecrest earthquake. At stations close to the rupture, the waveforms are diminished following the earthquake, with the autocorrelation eventually reverting to its pre-mainshock state within one month while distant stations show little to no evidence of the earthquake occurring. A similar trend was observed by Obermann et al. (2015), where fluid injections caused a loss of waveform coherence and was thought to be tied to changes of the scattering properties in the medium.

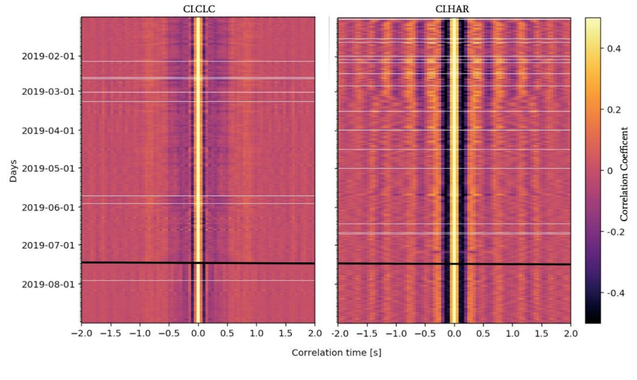

Figure 2: Stack of hourly autocorrelations for stations CI.CLC and CI.HAR. Color coded based on correlation coefficient between the daily correlations and the average correlation spanning from January to September 2019. The solid black line represents the M_w 7.1 Ridgecrest earthquake.

Temporal Seismic Velocity Variations

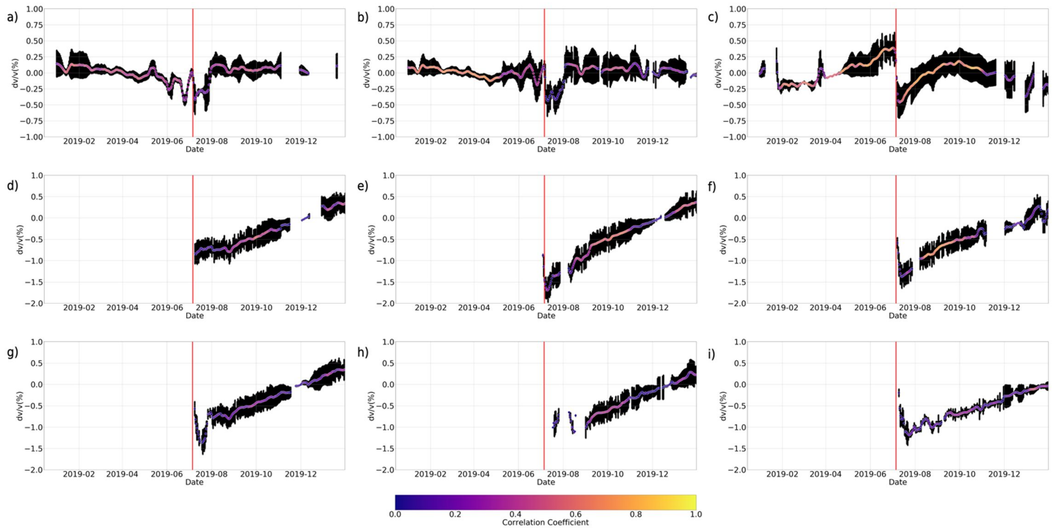

Figure 3: The annual temporal variations in seismic velocity (dv/v) for the CI and ZY stations during 2019 and 2020; a) CI. CCC, b) CI.CLC, c) CI.SRT, d) ZY.SV01, e) ZY.SV03, f) ZY.SV04, g) ZY.SV06, h) ZY.SV07, and i) ZY.SV08. Colors represent the correlation coefficients of the daily and reference autocorrelations, with their associated standard deviation shown in black. The red vertical line represents time of the M_w 7.1 Ridgecrest earthquake.

Nine of the stations experienced maximum velocity changes of 0.45% to 1.8%, relative to the *dv/v* values immediately before the M_w 7.1 Ridgecrest earthquake. Of the remaining seven stations, five (CI.SHO, CI.HAR, CI.TOW2, CI.WBS, and CI.LRL) either showed no perceptible response to the earthquake, remained relatively consistent over the time period, or exhibited a high level of background *dv/v* variation that made it impossible to identify changes associated with the Ridgecrest earthquake. Three of these stations (CI.SHO, CI.HAR and CI.WBS) are over 50 km away from the epicenter of the earthquake. Two stations (ZY.SV02 and ZY.SV05) had large amounts of missing data, which prevented them from being used in this study.

For the nine stations that had observable velocity changes, two recovery periods were observed, with *dv/v* values recovered to background levels within either one or three months. The seismic velocity at stations CI.SRT and ZY.SV01–8 took about three months to recover to a stable level. In contrast, stations CI.CCC and CI.CLC saw their velocities recover within about one month after the Ridgecrest earthquake. The longer recovery time appears to follow a steady *dv/v* increase over time period, while the one-month recovery for stations CI.CCC and CI.CLC did not initiate until late in the process, and recovery occurred over a short time period.

Distance and Ground-Motion Dependence of the Seismic Velocity Variations

The maximum velocity changes correlations strongly with the distance to the fault surface. Similarly each site's dynamic peak strain and *dv/v* measurements exhibit a linear correlation with greater velocity changes at the sites that experienced higher dynamic peak strains than at sites with lower peak strains. In addition, the *dv/v* measurements had a larger decreases closer to the rupture surface (Rrup). FInally, the *dv/v* measurements as a function of peak horizontal ground accelerations (PGA) indicate a weak correlation, with greater velocity changes at the sites that experienced stronger shaking.

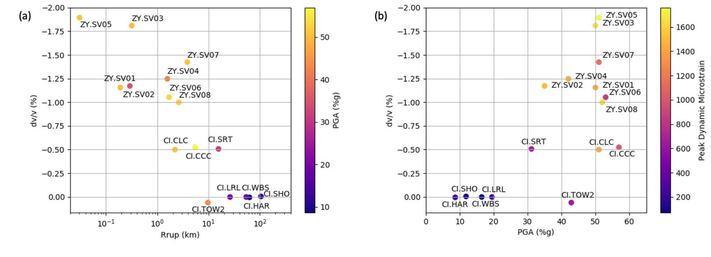

Figure 4: Scatterplot of the station parameters used in this study. A) Scatterplot of the temporal velocity variations (dv/v) for the 16 stations used in this study as a function of the closest distance to the rupture surface (Rrup). B) Scatterplot of the temporal velocity variations (dv/v) as a function of PGA of the M_w 7.1 earthquake. C) Scatterplot of the temporal velocity variations (dv/v) as a function of peak dynamic microstrain. The ZY stations values represent the upper limits due to the stations being installed days after the earthquake.

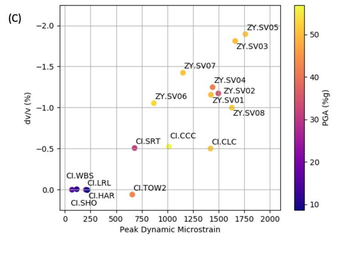

Conclusion

In this study, we investigated the temporal change and spatial patterns of the seismic velocity associated with the M_w 7.1 Ridgecrest earthquake. The observed velocity changes and differing recovery trends indicate that the area surrounding the Ridgecrest fault zone and near the Garlock fault experienced months-long modifications to the seismic velocity structure, with substantial recovery within three months. In all, we see evidence of the properties of the subsurface being altered by the mainshock in the region between the Ridgecrest fault zone and Garlock fault.

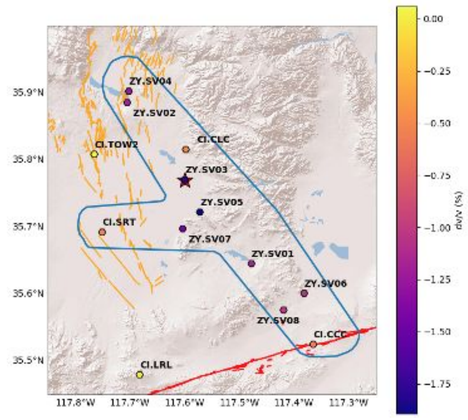

Figure 5: Zoomed in area between the Ridgecrest fault zone (orange) and Garlock fault (red) with the stations color coded based on their apparent velocity changes associated with the M_w 7.1 Ridgecrest earthquake. The 780 km^2 area of suspected of being altered by the M_w 7.1 Ridgecrest earthquake is outlined in blue.

References

- Cochran, E. S., Wolin, E., McNamara, D. E., Yong, A., Wilson, D., Alvarez, M., van der Elst, N., McClain, A., Steidl, J. (2020), The U.S. Geological Survey's Rapid Seismic Array Deployment for the 2019 Ridgecrest Earthquake, *Seismological Research Letters*.
- Hunter, J. (2007), Matplotlib: A 2D graphics environment, *Computing in Science & Engineering*, **9**(3), 90–95.
- Obermann, A., Kraft, T, Larose, E., and Wiemer, S. (2015), Potential of ambient seismic noise techniques to monitoring the St. Gallen geothermal site (Switzerland), *Journal of Geophysical Research: Solid Earth*, **120**,4301–4316.
- Rekoske, J. M., Thompson, E. M., Moschetti, M. P., Hearne, M. G., Aagaard, B. T., & Parker, G. A. (2020). The 2019 Ridgecrest, California, Earthquake Sequence Ground Motions: Processed Records and Derived Intensity Metrics. *Seismological Research Letters*.
- Sens-Schönfelder, C., and Wegler, U. (2006), Passive image interferometry and seasonal variations of seismic velocities at Merapi Volcano, Indonesia, *Geophysical Research Letters*, **33**(21).

Acknowledgements

Seismograms used in this study were collected using ObsPy, an open-source project dedicated to providing a Python framework for processing seismological data. The data used in this study were obtained from the Southern California Earthquake Data Center (SCEDC) at www.scedc.caltech.edu/research-tools and the IRIS Data Management Center at www.iris.edu under network codes CI (doi: 10.17914/SN/CI) and ZY (last accessed December 2019). The individual station parameters (PGA and PGV) were measured from the U.S. Geological Survey ShakeMap ,https://earthquake.usgs.gov/earthquakes/eventpage/ci38457511/shakemap/pga ,while the Vs^{30} values were measured using the U.S Geological Survey Vs30 Map viewer app, https://usgs.maps.arcgis.com/apps/webappviewer/index.html?id=8ac19bc3347f47e4865505f2837578e1. The values for Rrup were obtained from Rekoske et al. (2020). The data processing and measurements in this study were made using the Monitoring and Imaging based on Interferometric concepts package (www.github.com/miic-sw/miic). Figures were made using Matplotlib, a Python 2D plotting library, www.https://matplotlib.org (Hunter (2007)).

SAINT LOUIS UNIVERSITY EST. 1818

ObsPy A Python Framework for Seismology

IRIS

matplotlib

USGS science for a changing world